



Published in final edited form as:

*Clin Imaging*. 2018 ; 52: 106–112. doi:10.1016/j.clinimag.2018.07.007.

## Three-Dimensional Analysis of Regional Right Ventricular Shape and Function in Repaired Tetralogy of Fallot Using Cardiovascular Magnetic Resonance

S. Javed Zaidi<sup>1</sup>, Waseem Cossor<sup>1</sup>, Amita Singh<sup>2</sup>, Francesco Maffesanti<sup>2</sup>, Keigo Kawaji<sup>2</sup>, Joyce Woo<sup>2</sup>, Victor Mor-Avi<sup>2</sup>, David A. Roberson<sup>1</sup>, Shelby Kutty<sup>3</sup>, Amit R. Patel<sup>2</sup>

<sup>1</sup>Cardiology, Advocate Children's Hospital, Chicago IL

<sup>2</sup>Cardiology, University of Chicago Medicine, Chicago, IL

<sup>3</sup>University of Nebraska / Creighton University Children's Hospital, Omaha, Nebraska

### Abstract

**Background.**—Patients with surgically repaired Tetralogy of Fallot (rTOF) often have residual pulmonic valve regurgitation, leading to abnormal remodeling and dysfunction of the right ventricle often requiring pulmonic valve replacement. We tested the hypothesis that 3D analysis of right ventricular (RV) shape and function may reveal differences in regional adaptive remodeling that occurs in patients with rTOF, depending on whether a transannular patch (TAP) was utilized.

**Methods.**—Forty patients with rTOF who underwent cardiac magnetic resonance imaging (1.5T), including 20 with and 20 without TAP, and 10 normal controls were studied. Images were analyzed to measure RV endocardial curvature and global and regional volume and function.

**Results.**—RV ejection fraction (EF) was  $42\pm 11\%$  in TAP and  $38\pm 9\%$  in no-TAP ( $p=0.19$ ), both lower than  $54\pm 3\%$  in controls ( $p<0.01$ ). Left ventricular (LV) EF was  $54\pm 9\%$  in TAP,  $54\pm 8\%$  in no-TAP ( $p=0.87$ ) and  $61\pm 16\%$  in controls (both  $p<0.01$ ). Indexed LV end-diastolic volumes were higher in no-TAP than in TAP subgroup ( $p=0.02$ ). With TAP, mid RV septum showed lower curvature during diastole (less convex), than the mid and apical free walls and free wall adjacent to the RV outflow tract (RVOT; more convex). There were no differences in curvature during systole between rTOF subgroups but mid and RVOT free walls showed higher curvature versus controls.

**Conclusions.**—This is the first study to comprehensively describe the influence of TAP on changes in regional RV shape in patients with rTOF. Understanding these differences may help guide therapeutic options for residual pulmonary valve regurgitation in rTOF patients.

---

**Address for Correspondence:** Amit R. Patel, MD, University of Chicago, 5758 S. Maryland Avenue, MC9067, Chicago, IL 60637, amitpatel@uchicago.edu Phone: 773.702.1842.

**Disclosure:** The study was supported by a CTSA Pilot Award from the Institute of Translational Medicine (NIH Grant UL1 RR024999). Research support for other projects from Philips (ARP, KK, RML).

**Conflicts of interest:** None.

**Publisher's Disclaimer:** This is a PDF file of an unedited manuscript that has been accepted for publication. As a service to our customers we are providing this early version of the manuscript. The manuscript will undergo copyediting, typesetting, and review of the resulting proof before it is published in its final citable form. Please note that during the production process errors may be discovered which could affect the content, and all legal disclaimers that apply to the journal pertain.

## Keywords

congenital heart disease; right ventricle; 3D shape analysis; pulmonary valve; transannular patch

---

## Introduction

Advances in medical and surgical care of patients with tetralogy of Fallot (TOF) have led to excellent long-term survival with relatively low morbidity. Chronic re-intervention on the pulmonary valve and pulmonary arteries is now typical in this population. The earliest repairs performed in TOF included a large non-valved right ventricular (RV) outflow tract (RVOT) patch through the pulmonary valve annulus (traditional transannular patch (TAP)), leaving patients with severe pulmonary insufficiency (PI) <sup>1</sup>. This was thought to be benign and well tolerated. Unfortunately, this was found to be untrue, with patients at times developing akinesis/dyskinesis of the RVOT, patch aneurysms, RV free wall fibrosis, RV diastolic dysfunction, ventricular arrhythmias, conduction delays and even left ventricular (LV) dysfunction, all sequelae of chronic PI <sup>2-6</sup>. The non-valved TAP technique for repair of RVOT obstruction in TOF has been associated with poorer outcomes <sup>7, 8</sup>. Accordingly, the current focus has shifted to avoid non-valved TAP and to attempt surgical techniques sparing the pulmonary valve or providing pulmonary valve cusp augmentation <sup>9-11</sup>. Irrespective of this paradigm strategy shift, we currently continue to encounter adults with both types of TOF repair.

In patients with RV volume overload secondary to PI, cardiovascular magnetic resonance (CMR) is the reference standard for evaluation of RV volume and function <sup>12, 13</sup>. Optimal timing for initial or repeat intervention on the pulmonary valve for TOF, which is based on these measures remains controversial. However, serial longitudinal assessment of PI and RV function are an essential part of the medical care for TOF patients. One challenge with measurements of RV function is the complex three-dimensional (3D) shape of the right ventricle, which makes accurate RV volume measurements challenging. Furthermore, regional RV function, which may provide relevant information, is not commonly assessed because of the lack of suitable tools <sup>14</sup>. It is also unknown whether or how the surgical repair influences the complex RV shape and whether these changes are related to the type of surgery.

The 3D shape and function of the inflow, trabecular, and outflow RV regions may differ in patients with repaired tetralogy of Fallot (rTOF), according to the type of surgery performed. We hypothesized that patients with a TAP would have a generally more enlarged and convex right ventricle and larger changes in regional function and shape, as compared to patients with no TAP and normal controls. Accordingly, we studied changes in RV endocardial surface curvature and regional volume and function in patients with rTOF with and without TAP and compared them to each other as well as to normal subjects.

## Materials and Methods

### Study population

Forty patients who underwent CMR for evaluation of rTOF in three medical centers were retrospectively identified from cardiology databases, including two groups characterized as those repaired with a TAP (rTOF TAP) and those without a TAP (rTOF no TAP). A third group of ten normal subjects were added as controls. These control subjects were referred for a clinical CMR exam but had no obvious abnormalities detected. Patients with TOF with pulmonary atresia, absent pulmonary valve or placement of right ventricle to pulmonary artery conduit, as well as patients with residual pulmonary valve stenosis or pulmonary valve peak velocity  $>2$  m/sec (on pre-MRI echocardiography), were excluded. A chart abstraction was performed for demographic data. The study was approved by the Institutional Review Board of each participating institution.

### CMR image acquisition

CMR imaging was performed on clinical 1.5T scanner systems (Philips, General Electric, Siemens) with a 5-channel cardiac coil. Electrocardiogram-gated steady-state free-precession short-axis cine images (~30 phases per cardiac cycle) spanning from the apex to above the ventricular base, as well as long-axis images in the 4-chamber and RV 3-chamber planes were obtained. Typical imaging parameters were: echo time: 1.25msec, repetition time: 2.5msec, flip angle:  $60^\circ$ , slice thickness: 6 mm with 4 mm gaps, resolution varying from  $1.25 \times 1.25$  to  $1.79 \times 1.79$  mm (cine CMR).

### 3D endocardial surface analysis

The endocardial surface of the right ventricle was manually traced in the 4-chamber, RV 3-chamber, and short axis planes at end-diastole and end-systole using commercial software (3D RV Analysis, TomTec Imaging Systems, Unterschleissheim, Germany) to generate a 3D model of the RV cavity (Figure 1). This 3D endocardial surface model was saved as a connected mesh for further analysis.

### RV regional volume analysis

The RV surface model was divided into three distinct regions (Figure 2) using custom software: (1) the inlet region that extends from the atrioventricular junction to the chordal insertions, approximately  $2/3$  the distance from the base to the apex; (2) the trabecular region defined by muscle bundles traversing the chamber from septum to free wall, and (3) the outflow region made up of a smooth collar of myocardium known as the conus. In patients with rTOF TAP, the boundary between the RVOT and RVOT patch was identified based on the beginning of the dyskinetic inferior margin of the patch. To create these three regions, the 3D endocardial surface model was first divided into three equal-height segments from base to apex, and then further divided into anterior and posterior regions (Figure 2B). The basal and middle posterior segments were combined and labeled as the inlet region (Figure 2C; green compartment). The basal anterior segment was labeled as the outflow region (Figure 2C; blue compartment). The remaining three segments were labeled as the trabecular region (Figure 2C; red compartment).

## Endocardial surface curvature analysis

First, for each node on the connected mesh representing the RV endocardial surface, a quadratic polynomial function was locally fitted to approximate a smooth surface using a previously described technique<sup>15</sup>. Then, for each point, two values were calculated: maximum curvature  $k_1$ , defined as the inverse of the radius of a circle that would most closely fit the surface at that particular point, and the curvature  $k_2$ , similarly defined in the perpendicular direction. Then, local 3D surface curvedness,  $C$ , was calculated as the root mean square value of  $k_1$  and  $k_2$  and then normalized by mean instantaneous RV curvedness, calculated by averaging curvedness at all nodes on the endocardial surface. This latter step was performed to compensate for changes in RV regional shape secondary to changes in RV size.

Regional 3D normalized curvedness was obtained for each of the 3 regions defined above for the RV volume calculations by averaging local  $C$ -values measured in all nodes in the corresponding region. Data from nodes in direct continuity with the border between septum and free wall (Figure 2C, gray areas) were discarded to eliminate the effect of sharp curvature at the inflection points. The normalized curvedness,  $C_n$ , was mapped onto the volume-rendered endocardial surface for easy visualization of curvature information (Figure 2D).

Reproducibility was assessed by repeated measurements performed on 10 randomly selected subjects by the same operator one week apart. Inter-measurement variability was expressed in terms of absolute differences between the pairs of repeated measurements in percent of their mean.

## Statistical analysis

Measurement results were expressed as mean  $\pm$  SD. Normality of distribution of continuous variables was assessed using the Kolmogorov-Smirnov test and the distribution of all measured parameters was found to be close to normal. Global and regional RV volumes as well as septal and free-wall curvature for each region were calculated in subjects with rTOF and compared to normal controls, as well as between the two subgroups of rTOF patients using unpaired two-tailed student's  $t$ -test. A  $p$ -value  $<0.05$  was considered statistically significant.

## Results

### Demographics

The age range of rTOF patients was  $18\pm 4$  years and controls were  $21\pm 2$  years of age. The age at TOF repair was  $4\pm 3$  months for rTOF TAP subgroup and  $7\pm 9$  months for rTOF no TAP ( $p=0.29$ ). 70% of the patients and 40% of the controls were males. None of the patients had pulmonary valve stenosis, as evidenced by peak velocity  $<2$  m/sec in every patient. Pulmonary valve insufficiency was present in all subjects with rTOF, ranging from trace to severe. All controls had normal cardiovascular anatomy and function. Demographic characteristics of the study subjects are summarized in Table 1.

### Cine CMR Global Measurements

Global RV ejection fraction (EF) was reduced in both the rTOF subgroups and not statistically different ( $42\pm 11\%$  in rTOF TAP and  $38\pm 9\%$  in rTOF no TAP ( $p=0.19$ ). Global LV EF was similar in the rTOF subgroups:  $54\pm 9\%$  in rTOF TAP, and  $54\pm 8\%$  in rTOF no TAP groups ( $p=0.87$ ) and  $61\pm 16\%$  in the control group. The RV and LV EF and end-diastolic and end-systolic volume indices are shown in Table 2. There were no significant differences among the two rTOF subgroups in the indexed RV end-diastolic, RV end-systolic and LV end-systolic volumes. There was a difference in indexed LV end-diastolic volumes among the rTOF subgroups with the rTOF no TAP subgroup having higher volumes ( $p=0.02$ ).

### Regional Functional Analysis

Table 3 shows the summary of regional RV volume and function indices. RVOT EF was higher in patients with rTOF TAP when compared to rTOF no TAP. RV apical and RV inflow tract (RVIT) EF were similar in the rTOF subgroups. The latter was relatively more preserved than other RV regions. Indexed RVIT volumes were not statistically different between the rTOF subgroups. Indexed RV apical volumes were similar in both rTOF subgroups. Indexed RVOT volumes were higher in rTOF TAP as compared to no TAP.

### Regional Right Ventricular Shape

Intra-observer variability for curvedness measurements was 4%. The mid RV septum showed lower curvature during diastole (less convex, directed towards the RV), while the mid and apical free walls and the free wall adjacent to the RV outflow tract (RVOT) had higher curvature (more convex, directed outward from the RV) in patients with TAP (Figure 3). There were no significant differences in curvature patterns during systole between the two rTOF subgroups. The septum (RVIT and apex) and mid and RVOT free walls showed greater curvature in systole in the rTOF subgroups compared to controls. The diastolic and systolic curvature indices are summarized in Tables 4 and 5, respectively.

### Discussion

Complete repair of tetralogy of Fallot usually entails either a transannular patch (TAP) or valve sparing surgical interventions. Residual hemodynamic lesions after repair of TOF are variable and depend on the surgery performed. Most commonly, patients have residual pulmonary insufficiency (PI) or a combination of pulmonary stenosis (PS) and PI. The goal of repair is to minimize both PS and PI. The influences of the type of surgery on the subsequent changes in RV shape have not been well defined. Furthermore, adaptive remodeling in different regions of the RV may vary based on the surgery performed. Therefore, characterization of the differences in the 3D shape and function of various regions of the RV may provide new insight into these processes. Our study focused on studying the changes in RV endocardial surface curvature and regional volume and function in patients with rTOF with and without TAP.

Gupta et al., have surmised that the use of TAP can be avoided in almost two thirds of patients and may influence freedom from early RVOT re-intervention<sup>16</sup>. Survival in rTOF

has increased over the last several decades to over 90%<sup>17</sup> due to advances in surgical techniques and postoperative care. Following complete repair, patients often need re-intervention in the form of surgical or trans-catheter pulmonary valve placement/replacement. The timing of this intervention and the multi-modality imaging techniques utilized to reach an end-point has been controversial.

Previous authors have demonstrated changes in RV regional volume and function in rTOF, compared to normal controls using 3D echocardiography and CMR<sup>18, 19</sup>. Zhong et. al. described changes in endocardial surface curvature in rTOF as well, albeit using 2D methodology<sup>20</sup>. However, 2D analysis of RV curvature from CMR images is view-dependent and thus prone to considerable variability. To our knowledge, this is the first study to comprehensively describe these changes using 3D analysis of CMR images in a cohort of patients with rTOF in comparison with normal controls. Our results showed that there was RV dysfunction, as expected, in both groups but the difference in global RV function between the rTOF subgroups was not significant. Curvature differences were noted in three regions in diastole: the mid free wall, the apical free wall, and the free wall adjacent to the RVOT, suggesting that in patients with TAP, there is mild enlargement and subtle outward remodeling of the RV in these regions, sparing the entire RV inflow tract.

It is important to note that regional RV shape analysis is not designed to determine whether there is active remodeling in the RV regions that are most enlarged or if there is intrinsic cellular remodeling. There may have been presurgical RV shape changes, post surgical changes in shape due to the VSD patch or simply volume overload from PI. Similar to previous studies, we found that the largest RV regional enlargement occurs in the apical and outflow regions, sparing the inflow region. Leonardi et al showed that PI is associated with RV enlargement with bulging of the RV outflow tract and dilation of the RV apex<sup>21</sup>. We also found that the majority of this enlargement occurs in the mid and apical RV and outflow region in diastole. In normal subjects, these regions conform to the long crescent shape of the RV. As they enlarge in subjects with rTOF secondary to PI and/or RV dysfunction, they become substantially larger and more spherical structures. Conversely, the inflow region had little to no significant change in either volume or shape. These changes in the mid and apical RV and outflow regions pathophysiologically relate to volume overload from PI.

In addition to a global decrease in RV EF, global LV EF was decreased in rTOF patients as compared to normal controls. This is presumably secondary to inter-ventricle interactions with the enlarging dysfunctional RV effecting the function of the LV. Li et al., showed that, compared with the control subjects, global and regional RV longitudinal strain and strain rate and global LV longitudinal strain and strain rate, as well as LV circumferential and radial strain and strain rate were reduced in patients with rTOF<sup>22</sup>. Other studies have reported similar findings<sup>23, 24</sup>. In our study, RV indexed volumes were higher in the rTOF groups than normal subjects, also as expected, and likely secondary to the chronic volume overload prior to surgery followed by volume overload from PI following repair. We found no differences among the two rTOF subgroups in the indexed RV end-diastolic, RV end-systolic and LV end-systolic volumes.



Overall, free-wall normalized curvature was higher in subjects with rTOF. This is largely the result of the change in shape of the RV mid, apical and outflow regions, causing the average shape of these parts of the right ventricle to be more spherical. The overall average septal curvature in rTOF was more convex, while it was less convex in controls. This finding is somewhat counter-intuitive if one subjectively evaluates septal curvature based solely on short-axis slices. In the short-axis views, the septum appears somewhat flattened in rTOF patients compared to controls, but still concave. However, if one evaluates the 3D projection of septal curvature generated by our software, it is apparent that the septum becomes more saddle-shaped in rTOF. It is slightly concave in the short-axis view and slightly convex in the long-axis view. The long-axis convexity is most apparent near the outflow region (the region of the ventricular septal defect [VSD] patch in rTOF TAP) which takes on a more spherical shape. This pattern is not seen in all patients with rTOF, but is striking in those with the most RV enlargement. Diastolic curvatures in the apex, and RVOT free walls increased from the normal to the rTOF no TAP subgroup and was maximum in the TAP subgroup. The presence of this outward remodeling in both rTOF subgroups suggests that this remodeling occurs independently of the VSD patch.

The remodeling process, which results in changes in shape and regional volume, also has a significant effect on regional function. We found that the inflow region has the most preserved EF presumably due to minimal change in shape with RV enlargement. The areas with the largest change in shape, namely the mid, apical and outflow (free walls) have the most significant decline in regional EF. The apical and outflow regions therefore contribute less than normal to stroke volume. As a result of preserved EF, the inflow region may contribute more than the enlarged regions to help preserve RV stroke volume.

Our method of RV segmentation and differential analysis in terms of remodeling and ejection fractions may prove to be useful in patients with or without TAP to understand regional variations in global RV function. Sheehan et al., demonstrated that the right ventricle remodels in several directions, rather than following a shape continuum and that characterization of RV remodeling from 3D reconstructions provides novel insights<sup>18</sup>. Interestingly, despite this remodeling, the RVOT EF was higher in patients with TAP when compared to those without and no different than in normal subjects. This in contrast other studies that showed a decrease in RVOT EF in rTOF with TAP secondary to the non-contractile RVOT patch<sup>25</sup>. The theoretically increased PI with TAP could partially explain this difference in EF. However, we did not see statistically significant differences in PI in the subgroups with and without TAP, which may be secondary to inadequate statistical power. The enlarged RVOT in patients with TAP may also hold a larger blood volume than in normal controls or in patients with no TAP which could also increase the forward flow volume and consequently the EF. Also possibly secondary to our small sample size, statistical analysis of our variables in terms of correlations between RV curvedness, RVEF and PI fractions did not show significant associations. Additionally, patients with no TAP had surgery performed on average 3 months after patients with TAP. Although the difference was not statistically significant, it may be a clinically significant difference that could have influenced the findings. This may also explain why the LVEDV was higher in the no TAP group.

Pre-operative RVOT remodeling indices may prove beneficial in the current era where new surgical techniques emerge more frequently. Frigiola et al., have proposed that RV restoration (RVOT plasty) is a simple and effective procedure that introduces a structural component, which should be added during pulmonary valve implantation in patients with severe RV dilatation and underlying aneurysm or akinesia of the RVOT<sup>26</sup>. Though a routine CMR can detect RVOT aneurysm and akinesia, it cannot determine exactly which segments/walls of the RVOT could benefit from specific intervention. In particular, an enlarged RVOT prior to pulmonary valve replacement predicts suboptimal structural and functional outcomes<sup>27</sup> and our software is well suited to identify the specific areas needing additional surgical intervention during pulmonary valve replacement.

### Limitations

The present study evaluated a small sample of patients with rTOF with significant variations due to the timing of initial surgery, surgical repair strategy, and subsequent interventions. While one might view the size of our patient subgroups as too small, these groups were sufficiently large to detect significant differences in remodeling patterns. On the other hand, due to the small sample size, one cannot rule out type II errors, and thus our findings cannot be broadly generalized without future confirmatory findings.

Another potential limitation of our study is its retrospective nature. However, all the measurements and analyses were performed prospectively for the purposes of the study, without relying on values reported in patients' records. It is true that we used retrospectively acquired images, which would however not be any different had they been acquired prospectively.

Finally, in this study, RV volume and shape were measured only at end-systole and end-diastole, rather than throughout the cardiac cycle. As software tools that allow semi-automated frame-by-frame measurements of cardiac chamber volumes are being developed and validated, such analysis may in the future provide temporal indices of ventricular contraction and filling that may provide new insights into the cardiac physiology of patients with rTOF, especially the differences between patients with and without TAP. Similarly, dynamic analysis of segmental RV curvature may yield new information that would improve our understanding of this condition. However, the software we used in this study does not have this capability.

### Conclusions

To our knowledge, this is the first study to comprehensively describe the influence of TAP on changes in RV shape in patients with rTOF. We found mild enlargement and subtle outward remodeling in the region of the middle and apical free walls and the outflow regions of the right ventricle in patients with TAP. As new imaging modalities and surgical techniques emerge for treatment and follow up of patients with rTOF, there will certainly be more and more emphasis on subtle regional changes in segmental RV function (including hypokinesis and akinesia) and curvature. These changes may impact the selection of procedures used to treat residual pulmonary valve regurgitation in TOF patients such as the addition of RVOT plasty as proposed in some studies for the most enlarged right ventricles.



Further study of these changes may be useful to identify patients who may need earlier intervention and those who may have poor post intervention outcomes.

### Abbreviations:

<b>3D</b>	three-dimensional
<b>CMR</b>	cardiovascular magnetic resonance
<b>EF</b>	ejection fraction
<b>LV</b>	left ventricular
<b>PI</b>	pulmonary insufficiency
<b>PS</b>	pulmonary stenosis
<b>rTOF</b>	repaired tetralogy of Fallot
<b>RV</b>	right ventricular
<b>RVOT</b>	right ventricular outflow tract
<b>TAP</b>	transannular patch
<b>TOF</b>	tetralogy of Fallot
<b>VSD</b>	ventricular septal defect

### References

1. Sasson L, Houry S, Raucher Sternfeld A, Cohen I, Lenczner O, Bove EL, et al. Right ventricular outflow tract strategies for repair of tetralogy of Fallot: effect of monocusp valve reconstruction. *Eur J Cardiothorac Surg* 2013;43:743–51. [PubMed: 23024233]
2. Ilbawi MN, Idriss FS, DeLeon SY, Muster AJ, Gidding SS, Berry TE, et al. Factors that exaggerate the deleterious effects of pulmonary insufficiency on the right ventricle after tetralogy repair. Surgical implications. *J Thorac Cardiovasc Surg* 1987;93:36–44. [PubMed: 3796030]
3. Wald RM, Valente AM, Gauvreau K, Babu-Narayan SV, Assenza GE, Schreier J, et al. Cardiac magnetic resonance markers of progressive RV dilation and dysfunction after tetralogy of Fallot repair. *Heart* 2015;101:1724–30. [PubMed: 26276804]
4. de Ruijter FT, Weenink I, Hitchcock FJ, Meijboom EJ, Bennink GB. Right ventricular dysfunction and pulmonary valve replacement after correction of tetralogy of Fallot. *Ann Thorac Surg* 2002;73:1794–800; discussion 800. [PubMed: 12078771]
5. Hickey EJ, Veldtman G, Bradley TJ, Gengsakul A, Manlhiot C, Williams WG, et al. Late risk of outcomes for adults with repaired tetralogy of Fallot from an inception cohort spanning four decades. *Eur J Cardiothorac Surg* 2009;35:156–64; discussion 64. [PubMed: 18848456]
6. Gatzoulis MA, Balaji S, Webber SA, Siu SC, Hokanson JS, Poile C, et al. Risk factors for arrhythmia and sudden cardiac death late after repair of tetralogy of Fallot: a multicentre study. *Lancet* 2000;356:975–81. [PubMed: 11041398]
7. Luijten LW, van den Bosch E, Duppen N, Tanke R, Roos-Hesselink J, Nijveld A, et al. Long-term outcomes of transatrial-transpulmonary repair of tetralogy of Fallot. *Eur J Cardiothorac Surg* 2015;47:527–34. [PubMed: 24801339]
8. Nollert G, Fischlein T, Bouterwek S, Bohmer C, Klinner W, Reichart B. Long-term survival in patients with repair of tetralogy of Fallot: 36-year follow-up of 490 survivors of the first year after surgical repair. *J Am Coll Cardiol* 1997;30:1374–83. [PubMed: 9350942]

9. Hua Z, Li S, Wang L, Hu S, Wang D. A new pulmonary valve cusp plasty technique markedly decreases transannular patch rate and improves midterm outcomes of tetralogy of Fallot repair. *Eur J Cardiothorac Surg* 2011;40:1221–6. [PubMed: 21458290]
10. Anagnostopoulos P, Azakie A, Natarajan S, Alphonso N, Brook MM, Karl TR. Pulmonary valve cusp augmentation with autologous pericardium may improve early outcome for tetralogy of Fallot. *J Thorac Cardiovasc Surg* 2007;133:640–7. [PubMed: 17320558]
11. Attanawanich S, Ngodgnamthaweesuk M, Kitjanon N, Sitthisombat C. Pulmonary cusp augmentation in repair of tetralogy of Fallot. *Asian Cardiovasc Thorac Ann* 2013;21:9–13. [PubMed: 23430414]
12. Geva T. Repaired tetralogy of Fallot: the roles of cardiovascular magnetic resonance in evaluating pathophysiology and for pulmonary valve replacement decision support. *J Cardiovasc Magn Reson* 2011;13:9. [PubMed: 21251297]
13. Pennell DJ, Sechtem UP, Higgins CB, Manning WJ, Pohost GM, Rademakers FE, et al. Clinical indications for cardiovascular magnetic resonance (CMR): Consensus Panel report. *J Cardiovasc Magn Reson* 2004;6:727–65. [PubMed: 15646878]
14. Morcos M, Sheehan FH. Regional right ventricular wall motion in tetralogy of fallot: a three dimensional analysis. *Int J Cardiovasc Imaging* 2013;29:1051–8. [PubMed: 23292150]
15. Maffessanti F, Lang RM, Niel J, Steringer-Mascherbauer R, Caiani EG, Nesser HJ, et al. Three-dimensional analysis of regional left ventricular endocardial curvature from cardiac magnetic resonance images. *Magn Reson Imaging* 2011;29:516–24. [PubMed: 21216552]
16. Gupta U, Polimenakos AC, El-Zein C, Ilbawi MN. Tetralogy of Fallot with atrioventricular septal defect: surgical strategies for repair and midterm outcome of pulmonary valve-sparing approach. *Pediatr Cardiol* 2013;34:861–71. [PubMed: 23104595]
17. Bacha EA, Scheule AM, Zurakowski D, Erickson LC, Hung J, Lang P, et al. Long-term results after early primary repair of tetralogy of Fallot. *J Thorac Cardiovasc Surg* 2001;122:154–61. [PubMed: 11436049]
18. Sheehan FH, Ge S, Vick GW 3rd, Urnes K, Kerwin WS, Bolson EL, et al. Three-dimensional shape analysis of right ventricular remodeling in repaired tetralogy of Fallot. *Am J Cardiol* 2008;101:107–13. [PubMed: 18157975]
19. Bodhey NK, Beerbaum P, Sarikouch S, Kropf S, Lange P, Berger F, et al. Functional analysis of the components of the right ventricle in the setting of tetralogy of Fallot. *Circ Cardiovasc Imaging* 2008;1:141–7. [PubMed: 19808531]
20. Zhong L, Gobeawan L, Su Y, Tan JL, Ghista D, Chua T, et al. Right ventricular regional wall curvedness and area strain in patients with repaired tetralogy of Fallot. *Am J Physiol Heart Circ Physiol* 2012;302:H1306–16. [PubMed: 22210750]
21. Leonardi B, Taylor AM, Mansi T, Voigt I, Sermesant M, Pennec X, et al. Computational modelling of the right ventricle in repaired tetralogy of Fallot: can it provide insight into patient treatment? *Eur Heart J Cardiovasc Imaging* 2013;14:381–6. [PubMed: 23169758]
22. Li Y, Xie M, Wang X, Lu Q, Zhang L, Ren P. Impaired right and left ventricular function in asymptomatic children with repaired tetralogy of Fallot by two-dimensional speckle tracking echocardiography study. *Echocardiography* 2015;32:135–43. [PubMed: 24661011]
23. Fernandes FP, Manlhiot C, Roche SL, Grosse-Wortmann L, Slorach C, McCrindle BW, et al. Impaired left ventricular myocardial mechanics and their relation to pulmonary regurgitation, right ventricular enlargement and exercise capacity in asymptomatic children after repair of tetralogy of Fallot. *J Am Soc Echocardiogr* 2012;25:494–503. [PubMed: 22326134]
24. Koestenberger M, Ravekes W, Nagel B, Avian A, Heinzl B, Fritsch P, et al. Longitudinal systolic ventricular interaction in pediatric and young adult patients with TOF: a cardiac magnetic resonance and M-mode echocardiographic study. *Int J Cardiovasc Imaging* 2013;29:1707–15. [PubMed: 23820958]
25. Puranik R, Tsang V, Lurz P, Muthurangu V, Offen S, Frigiola A, et al. Long-term importance of right ventricular outflow tract patch function in patients with pulmonary regurgitation. *J Thorac Cardiovasc Surg* 2012;143:1103–7. [PubMed: 22056367]

26. Frigiola A, Giamberti A, Chessa M, Di Donato M, Abella R, Foresti S, et al. Right ventricular restoration during pulmonary valve implantation in adults with congenital heart disease. *Eur J Cardiothorac Surg* 2006;29 Suppl 1:S279–85. [PubMed: 16564697]
27. O’Meagher S, Ganigara M, Munoz P, Tanous DJ, Chard RB, Celermajer DS, et al. Right ventricular outflow tract enlargement prior to pulmonary valve replacement is associated with poorer structural and functional outcomes, in adults with repaired Tetralogy of Fallot. *Heart Lung Circ* 2014;23:482–8. [PubMed: 24345378]

**Highlights**

- 3D analysis of right ventricular shape and function revealed differences in regional adaptive remodeling in patients with repaired TOF with and without transannular patch.
- Understanding of these differences may affect the selection of procedures used to treat residual pulmonary valve regurgitation in TOF patients.

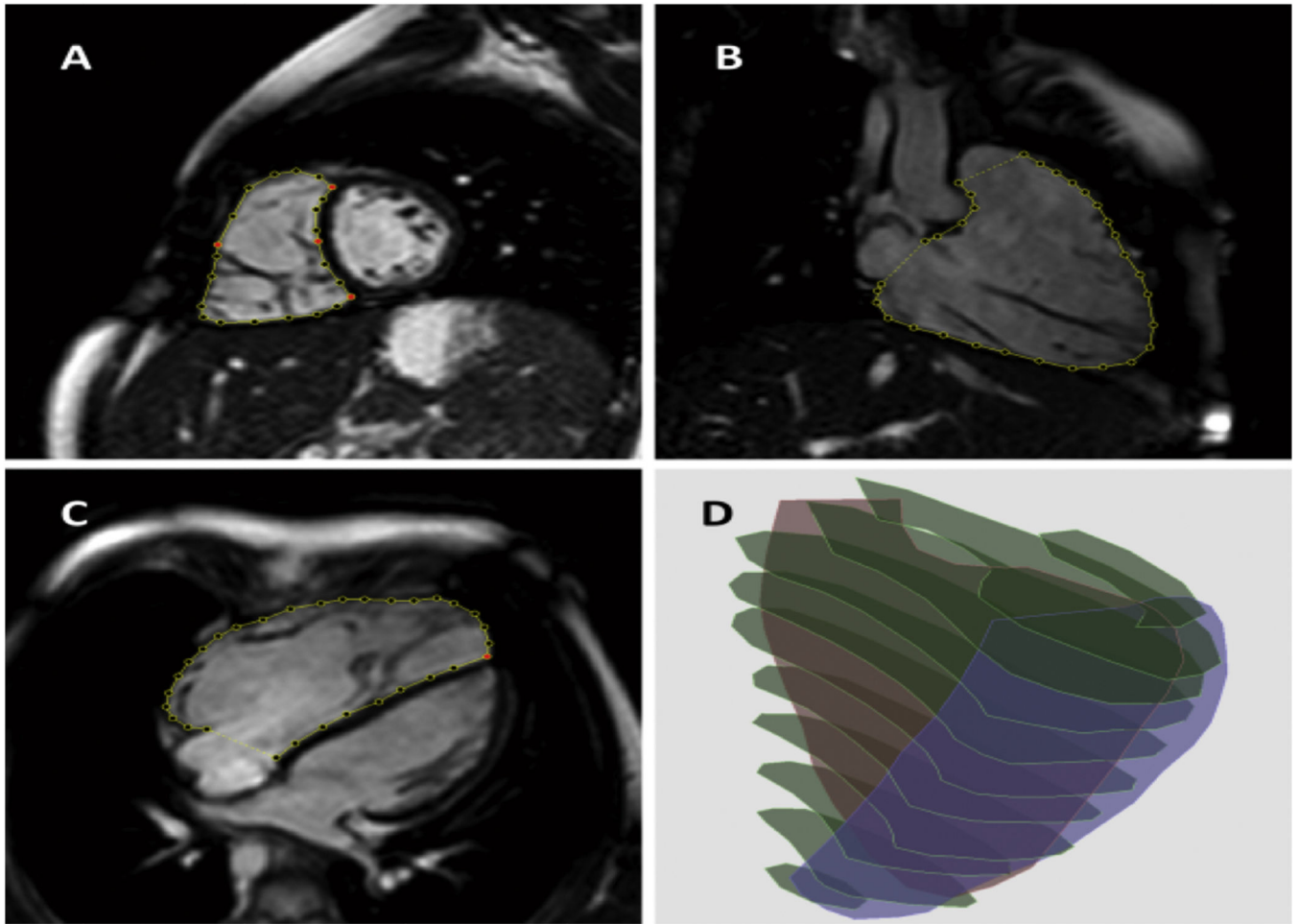


**Figure 1.** 3D reconstruction of the RV cavity. After RV boundaries are manually traced in a stack of short-axis (A), RV 3-chamber (B) and 4-chamber (C) views, the tracings are stacked in the 3D space to generate a 3D cast of the RV cavity (D).

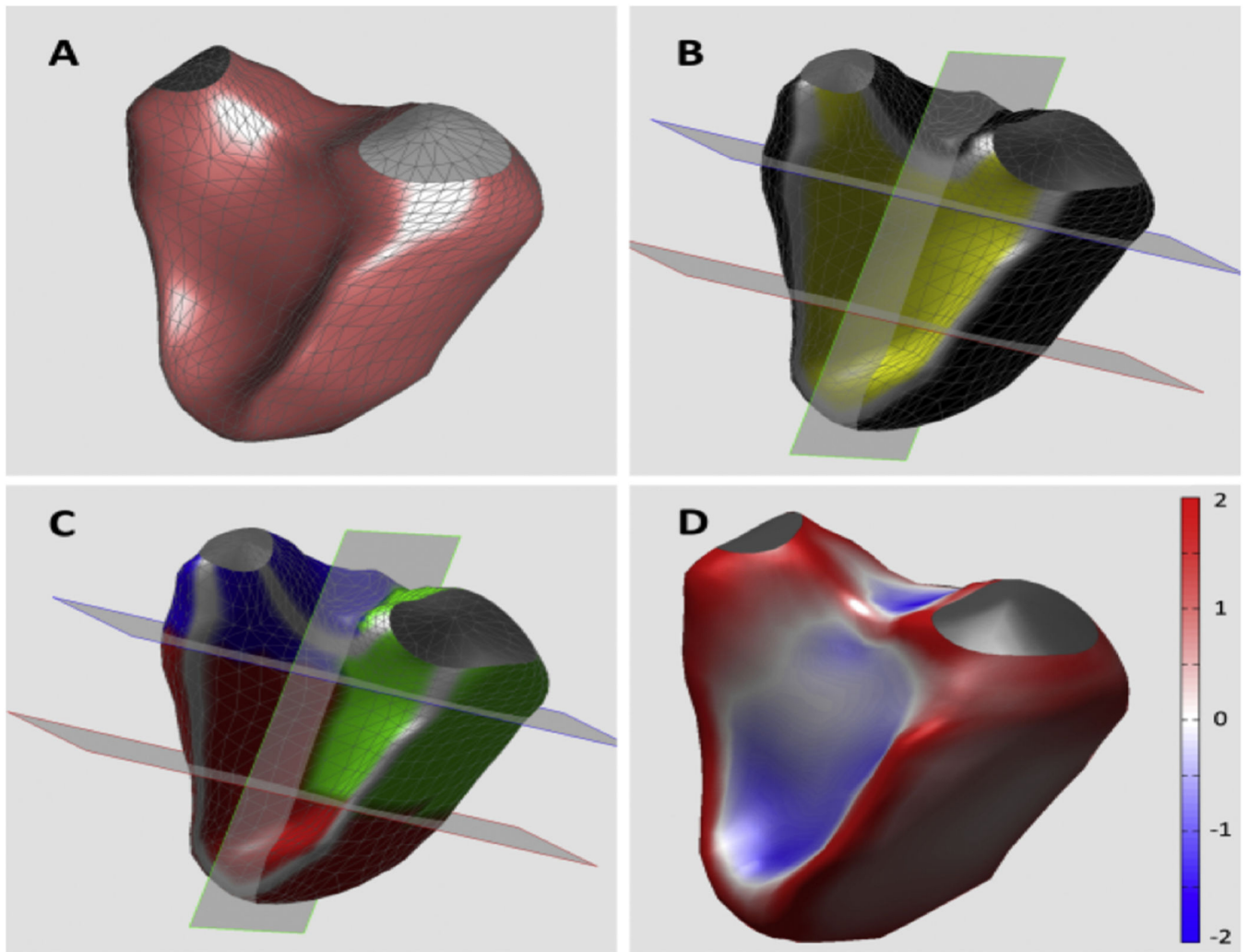


**Figure 2.** 3D analysis of regional RV volume and shape. Reconstructed 3D RV surface (A) was divided into 6 segments (B) and used to measure volumes in 3 RV regions: inlet (green), outflow (blue) and trabecular (red) regions (see text for details). Curvature was calculated for each point of the RV surface: see color-encoded RV cast (D).



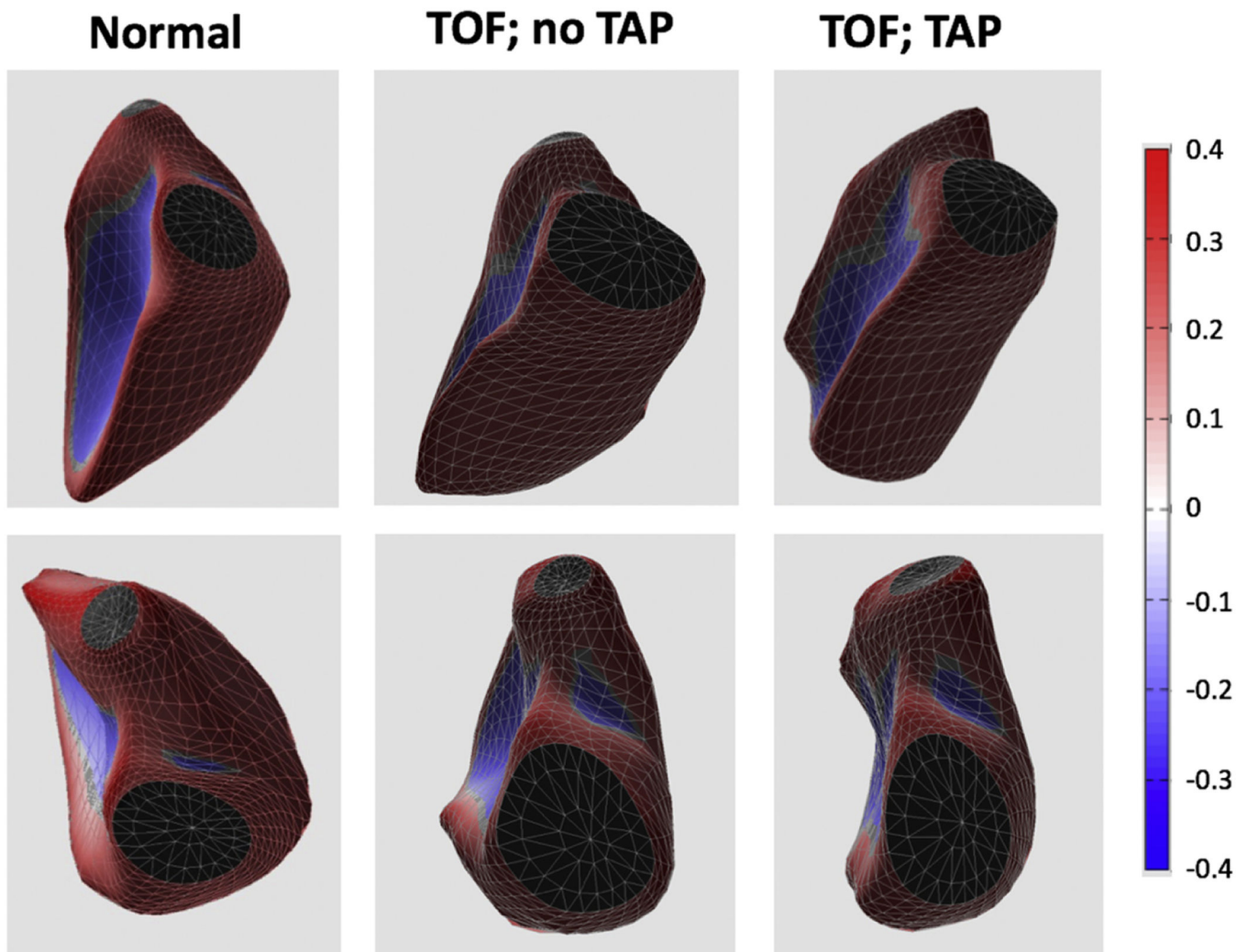


**Figure 3.** Examples of 3D casts of the RV cavity obtained in 3 subjects: normal control (left), and two rTOF patients: without (middle) and with (right) transannular patch (TAP). As the mid and apical free wall and the RVOT become more convex (top and bottom, respectively) among these three subjects (left to right), RV curvedness increases in a stepwise manner.

**Table 1:**

Demographic data.

	TAP (n=20)	No TAP (n=20)	Normal controls (n=10)
Age (years)	18 ± 4	20 ± 11	21 ± 2
Age at repair (months)	4 ± 3	7 ± 9	---
M/F (%)	70/30	50/50	40/60
BSA	1.5 ± 0.4	1.4 ± 0.5	1.8 ± 0.2

Author Manuscript

Author Manuscript

Author Manuscript

Author Manuscript

**Table 2:**

Global right and left ventricular measurements.

Ventricular Volumes	rTOF TAP	rTOF no TAP	Normals	P-value	P-value
				rTOF pts	NL vs. rTOF
RV EF (%)	43 ± 11	38 ± 9	55 ± 3	0.17	<0.01
RV EDVi (mL/m <sup>2</sup> )	137 ± 19	129 ± 29	84 ± 17	0.31	<0.01
RV ESVi (mL/m <sup>2</sup> )	78 ± 16	80 ± 24	42 ± 4	0.73	<0.01
LV EF (%)	54 ± 9	54 ± 8	60 ± 6	0.87	<0.01
LV EDVi (mL/m <sup>2</sup> )	76 ± 12	87 ± 17	87 ± 14	0.02	0.83
LV ESVi (mL/m <sup>2</sup> )	34 ± 8	40 ± 14	35 ± 8	0.10	0.35

RV EF: right ventricular ejection fraction; RV EDVi: indexed right ventricular end diastolic volume; RV ESVi: indexed right ventricular end systolic volume; LV EF: left ventricular ejection fraction; LV EDVi: indexed left ventricular end diastolic volume; LV ESVi: indexed left ventricular end systolic volume;

**Table 3:**

RV regional volumes and function

Ventricular Volumes		TAP	No TAP	Normal	P-value ToF	P-value normal vs. all TOF
RV Apical EF (%)		45 ± 12	40 ± 10	58 ± 10	0.23	<0.01
RVOT EF (%)		35 ± 14	17 ± 3	48 ± 10	0.02	<0.01
RVIT EF (%)		46 ± 12	44 ± 13	60 ± 1	0.61	0.04
Indexed RV Vol <sub>Apex</sub> (mL/m <sup>2</sup> )	Diastole	65 ± 11	61 ± 16	34 ± 9	0.42	<0.01
	Systole	36 ± 10	31 ± 18	14 ± 5	0.37	<0.01
Indexed RV Vol <sub>RVOT</sub> (mL/m <sup>2</sup> )	Diastole	18 ± 5	13 ± 6	12 ± 3	<0.01	<0.01
	Systole	12 ± 3	9 ± 5	6 ± 2	0.04	<0.01
Indexed RV Vol <sub>RVIT</sub> (mL/m <sup>2</sup> )	Diastole	55 ± 14	61 ± 18	38 ± 8	0.31	<0.01
	Systole	32 ± 7	29 ± 18	18 ± 4	0.54	<0.01
Pulmonic Insufficiency (RF %)		35 ± 18	29 ± 19	---	0.35	--

**Table 4:**

Diastolic curvature indices

	TAP	No TAP	Normal
<b>Septal Apex</b>	0.32 ± 0.18	0.35 ± 0.25	<b>0.11 ± 0.13<sup>#</sup></b>
<b>Septal RVIT</b>	1.21 ± 0.28	1.25 ± 0.29	1.18 ± 0.27
<b>Septal RVOT</b>	0.73 ± 0.22	0.79 ± 0.31	0.71 ± 0.06
<b>Mid Septum</b>	0.62 ± 0.08	<b>0.69 ± 0.08<sup>*</sup></b>	0.69 ± 0.08
<b>Free Wall Apex</b>	1.64 ± 0.09	<b>1.53 ± 0.14<sup>*</sup></b>	<b>1.33 ± 0.15<sup>#</sup></b>
<b>Free Wall RVIT</b>	1.74 ± 0.24	1.72 ± 0.28	1.64 ± 0.26
<b>Free Wall RVOT</b>	1.36 ± 0.09	<b>1.26 ± 0.08<sup>*</sup></b>	<b>0.87 ± 0.11<sup>#</sup></b>
<b>Mid Free Wall</b>	1.57 ± 0.05	<b>1.50 ± 0.11<sup>*</sup></b>	<b>1.16 ± 0.23<sup>#</sup></b>

\* p&lt;0.05 between ToF groups;

# p&lt;0.05 between normal and combined rToF groups

**Table 5:**

Systolic curvature indices

	TAP	No TAP	Normal
<b>Septal Apex</b>	0.29 ± 0.26	0.29 ± 0.20	<b>0.11 ± 0.10<sup>#</sup></b>
<b>Septal RVIT</b>	1.13 ± 0.21	1.20 ± 0.34	<b>0.52 ± 1.84<sup>#</sup></b>
<b>Septal RVOT</b>	0.75 ± 0.20	0.80 ± 0.39	0.84 ± 0.27
<b>Mid Septum</b>	0.67 ± 0.14	0.68 ± 0.22	0.76 ± 0.46
<b>Free Wall Apex</b>	1.54 ± 0.12	1.46 ± 0.38	1.47 ± 0.17
<b>Free Wall RVIT</b>	1.73 ± 0.21	1.52 ± 0.41	1.61 ± 0.79
<b>Free Wall RVOT</b>	1.30 ± 0.11	1.31 ± 0.13	<b>1.20 ± 0.10<sup>#</sup></b>
<b>Mid Free Wall</b>	1.47 ± 0.08	1.47 ± 0.09	<b>1.29 ± 0.29<sup>#</sup></b>

<sup>#</sup>p<0.05 between normal and TOF groups